

## Impact of a truck Driver's strike on air pollution levels in São Paulo

Júlio Barboza Chiquetto <sup>a,\*</sup>, Débora Souza Alvim <sup>b</sup>, José Roberto Rozante <sup>b</sup>, Marlon Faria <sup>c</sup>, Vinícius Rozante <sup>d</sup>, João Paulo Assis Gobo <sup>e</sup>

<sup>a</sup> Institute of Advanced Studies, University of São Paulo, Brazil

<sup>b</sup> Center for Weather Forecast and Climate Studies, National Institute for Space Research, Brazil

<sup>c</sup> Institute of Physics, University of São Paulo, Brazil

<sup>d</sup> School of Chemical Engineering, State University of Campinas, Brazil

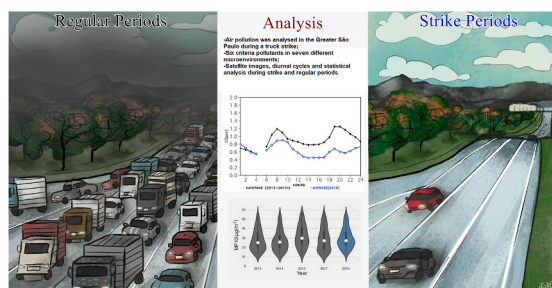
<sup>e</sup> Geography Department, Federal University of Rondônia, Brazil



### HIGHLIGHTS

- We evaluated the impact of a truck driver strike on air pollution in São Paulo.
- Primary pollutants (CO and NO) decreased by 50%, predominantly in roadside locations.
- NO<sub>2</sub>, PM<sub>10</sub>, and PM<sub>2.5</sub> showed mixed impacts while O<sub>3</sub> increased by 30%.
- Results help to understand the role of vehicular emissions in urban environments.
- Secondary reactions and atmospheric conditions are key factors in restriction periods.

### GRAPHICAL ABSTRACT



### ARTICLE INFO

#### Keywords:

Criteria pollutants  
Vehicular emission  
Urban microenvironments  
Truck strike  
Urban air pollution  
Diurnal cycle

### ABSTRACT

From May 21st to 31st, 2018, a truck driver strike greatly decreased all vehicle activity in Brazil. We evaluated the concentrations of criteria pollutants in seven different microenvironments during this period in the São Paulo Megacity. Results were evaluated by violin plots, the Kruskal-Wallis test and diurnal cycles, comparing the year 2018 to an average of 4 previous years. Primary pollutants (CO and NO) decreased by 50% in 2018, predominantly in roadside (RDS) locations. NO<sub>2</sub>, PM<sub>10</sub>, and PM<sub>2.5</sub> did not decrease as much, suggesting the relevance of secondary reactions and other sources (ex: fires). Ozone increased significantly (about 30–50%), possibly due to favourable atmospheric conditions (solar radiation) and changes in the NO<sub>x</sub>/VOCs ratio caused by the decrease in NO. Our findings help to better assess the role of vehicular emissions and provide insights on the impacts of interruption of activities (ex: during lockdowns) over air quality in metropolitan environments.

### 1. Introduction

The transportation sector is an important source of emission of hazardous air pollutants and greenhouse gases. In the Metropolitan Area

of São Paulo (MASP), light and heavy-duty vehicles emitted 97% of carbon monoxide (CO), 70% of the nitrogen oxides (NO<sub>x</sub>), 80% of hydrocarbons (HCs), 40% of the particulate matter (PM) and 16% of sulphur oxides (SO<sub>x</sub>), according to a report by the Environmental

\* Corresponding author. Rua da Praça do Relógio, 109, térreo, Cidade Universitária, 05508-050, São Paulo, SP, Brazil.

E-mail address: [julio22@usp.br](mailto:julio22@usp.br) (J.B. Chiquetto).

Agency of the State of São Paulo – CETESB (CETESB, 2018). Also, São Paulo was ranked as the 4th worst traffic jam worldwide, with people spending 2 h on average during their daily commute, leading to health burdens and economic losses, likely to reach billions of dollars (Cookson and Pishue 2017; Leirião et al., 2019). It has been estimated that heavy-duty vehicles (HDV) in São Paulo contribute to up to 47% of atmospheric black carbon (BC) and 40% of certain volatile organic compounds (VOCs, such as benzene and toluene).

However, public transport users occupy much less urban space and produce much lower emissions per capita than individual vehicle users (Sider et al., 2015). This shows how the urban environment is highly characterized by synergic fluxes, as changes in one sector (land use, transport) may well impact others (health, economy, environment, etc.). This points to the urgent need to better understand these complex interactions in the urban environment, particularly in the developing world, in order to implement governance and policy changes aiming more equitable, sustainable and resilient cities (Malik et al., 2019).

During the 21st-31st of May, in 2018, a nation-wide truck driver strike took place in Brazil. Truck drivers demanded a decrease in fuel prices and improvements on working conditions. This social mobilization paralyzed nearly all HDV circulation throughout Brazil. Because fuel delivery to gas stations is provided by trucks, this led to a shortage of most vehicle fuels – which in turn lead to an expressive decrease in the activity of light duty vehicles (LDV) as well. Traffic count in São Paulo during the strike period was reduced to figures as low as 2 km at rush hours during the strike. The municipal bus fleet was also decreased by nearly 50%, and part of the universities, schools and other services stopped their activities (see Table 1).

Previous studies concerning air quality and vehicular activity changes have demonstrated different impacts on pollutant concentrations. In India, a decrease of about 50% in carbon monoxide CO, BC, PM and ozone ( $O_3$ ) was observed during a nationwide truck strike (Sharma et al., 2010). In Italy and Spain, public transport strikes lead to a greater use of private vehicles and increased the concentrations of some pollutants (CO and HC), but for PM, results were more complex due to other sources and the secondary PM fraction (Meinardi et al., 2008; Basagaña et al., 2018). In Spain, the impact of these emission changes over ozone varied seasonally due to changes in atmospheric conditions and its complex atmospheric chemistry. In Israel, an analysis performed for a national holiday demonstrated a decrease of at least 80% in NO concentrations in different sites, while ozone increased about 8 ppbv in the urban core during the day and increased 20–30 ppbv during the night (Levy, 2013). Increases in ozone were also found in a study performed for Rio de Janeiro during the 2018 truck strike (Dantas et al., 2019). Similar increases were also found during the COVID-19 lockdown periods in Brazil, Spain and India, which altered vehicular emission in a comparable way (Siciliano et al., 2020; Mahato et al., 2020; Nakada and Urban, 2020; Tobías et al., 2020). It is then evident that changes in pollutant emission, such as in the truck driver's strike, are likely to have different spatial responses in pollutant concentrations according to the many different urban microenvironments across megacities, also revealing insights on population exposure (Levy et al., 2014). These results show that the relationship between the different social dynamics, emission patterns and pollutant concentrations is complex, and more studies are necessary to understand these relationships – particularly in the recent context of possible future lockdowns and activity interruption caused by pandemic situations.

The nationwide truck strike period created a natural laboratory with an absence of diesel-operated trucks and a great decrease in urban buses and also LDV. A recent study evaluating NO<sub>x</sub>, PM<sub>10</sub> and O<sub>3</sub> in downtown São Paulo during this strike was conducted but centred on health outcomes in four sites in downtown São Paulo (Leirião et al., 2020). We provide a different approach, analysing the concentrations of CO, NO, NO<sub>2</sub>, PM<sub>10</sub>, PM<sub>2.5</sub> and O<sub>3</sub> at seven ground monitoring stations in the MASP which represent downtown and urban background microenvironments during the period of the truck driver's strike in 2018. The

analysis was performed through different statistical analyses and diurnal cycles, compared to an average of the same period for previous years, when there was no strike. Results showed that the strike led to significant decreases in the primary air pollutants analysed, an increase in ozone and mixed results for PM and NO<sub>2</sub> compared to the average of the previous years. These findings are also in line with the results of recent studies evaluating air quality changes from lockdown measurements due the COVID-19 pandemic.

## 2. Data and methods

### 2.1. Air pollution data description

Hourly data for the period 21st – 31st of May 2018, and from the same period from the previous five years (2013–2017), were obtained at the CETESB online database, for CO, NO, NO<sub>2</sub>, PM<sub>10</sub>, PM<sub>2.5</sub> and O<sub>3</sub>. Seven monitoring sites from this network were chosen for analysis due to the following criteria: availability of data, quality of data (at least 75% of hourly the time series from the periods used), and exposure/land use representation: vehicular or roadside, commercial (mixed land use), residential and urban background, according to recommendations from the World Health Organization (WHO, 2000). This was important to make sure that the truck strike impacts were indeed observed across the megacity in different urban microenvironments. Data from stations located at the coast and the countryside were also obtained but included only as supplementary material (Supplementary material 1 and 2, and see Fig. 1 for a list of acronyms).

### 2.2. Atmospheric data and analysis

Precipitation, temperature and wind data from the Emergency Management Centre of the city of São Paulo were also used to assist the atmospheric analysis. Since atmospheric conditions can strongly impact pollutant concentrations, we also produced daily graphs of temperature, relative humidity and precipitation in order to assess the role of certain air masses with possible influence over pollutant concentrations. In a study conducted for the Metropolitan Area of São Paulo, Sánchez-Ccocylo and de Fátima Andrade (2002) observed that pollutant concentrations increased when high-pressure systems prevailed over the region, such as the Subtropical Atlantic High or extratropical high-pressure systems following cold fronts. These systems bring increased air pressure and stability, unfavourable conditions for the dispersion of pollutants. On the other hand, when cold front conditions prevailed, low pressure and higher atmospheric instability were associated to lower pollutant concentrations. A brief synoptic analysis was then performed in this study during the strike period in all years evaluated (21-31st of May 2013–2018) (section 3.1). To properly assess the truck driver's strike impact over pollutant concentrations, the periods analysed should have comparable atmospheric conditions, so the role of emission changes can be better disentangled from atmospheric conditions (sections 3.2 and 3.3). As a result, the year 2016, which presented distinct atmospheric conditions, was removed from the other procedures in this study (diurnal cycles, violin plots and statistical analyses). Therefore, we will refer to the period 2013–2017\* as the averages of 2013, 2014, 2015 and 2017 (without 2016).

### 2.3. Satellite images

Satellite imagery was obtained at different sources and used to obtain an average of the pollutant concentrations for the period of the strike in 2018, and the previous years of 2013–2017\*, centred over southeast Brazil. In order to assess the particulate matter, we used Optical Aerosol Depth (AOD) from the spectral radiometers MODIS (Moderate Resolution Imaging Spectroradiometer), aboard of American satellite Terra series EOS, which provides daily observations of AOD globally (Platnick et al., 2003). The MODIS (Terra) datasets used in this

study were downloaded at Level 3 from Atmosphere Archive and Distribution System (LAADS) Distributed Active Archive Centre (DAAC) website ([ladsweb.modaps.eosdis.nasa.gov](https://ladsweb.modaps.eosdis.nasa.gov)). Over continental areas, MODIS AOD uncertainty is  $\pm 0.05 \pm 0.15 \times \text{AODAERONET30}$ . As source information, we used daily averaged values combined Dark Target and Deep Blue AOD at 550 nm for land and ocean with space resolution  $1^\circ$  and 3 km. For  $\text{NO}_2$ , the data were obtained at the Giovanni NASA website, from the OMI sensor (Ozone Monitoring Instrument) from the Aura satellite (Leviet et al., 2006). Data were obtained from the wavelength 0.35–0.5  $\mu\text{m}$  (which corresponds to Band 3), Level-3, daily global gridded Nitrogen Dioxide Product ( $\text{OMNO}_2\text{d}$ ,  $0.25 \times 0.25^\circ$ ). This product contains Total Tropospheric Column  $\text{NO}_2$  for sky conditions where cloud fraction is less than 30 percent. Gridded CO *A priori* monthly data from Level 3 version 8 (V8) of the MOPITT (Measurement Of Pollution In The Troposphere), based on simultaneous thermal-infrared (TIR) and near-infrared (NIR) products from the mixing ratio of 1000 hPa is used. The TIR-NIR product offers the greatest vertical resolution and considerable sensitivity to CO in the lower troposphere, with accuracy around 10% (Edwards et al., 1999; Deeter et al., 2014). MOPITT products are available at <https://www2.acom.ucar.edu/mopitt>, and data can be downloaded at <https://earthdata.nasa.gov/>. We used this data to check if the impacts of the truck strike would be perceived on satellite images on a regional scale. We also obtained data about fires in the state of São Paulo during the same periods from the Brazilian National Space Research Institute (INPE) (<http://queimadas.dgi.inpe.br/queimadas/bdqueimadas/>).

#### 2.4. Air pollution data analysis

For the analysis of the hourly evolution of pollutants, we calculated diurnal cycles, by computing an average for each hour of the day in the period analysed. The following calculation was performed for each pollutant, at each hour of the day, leading to an averaged-24-h graph for each pollutant at all monitoring sites.

$$\bar{x}_i = \frac{x_{ij1} + x_{ij2} + \dots + x_{ijn}}{n}$$

where:  $\bar{x}_i$  = average for pollutant  $x$  at hour  $i$ , for each day  $j$  for an  $n$

number of days.

We compared the diurnal cycles of 2018 with diurnal cycles for the average of 2013–2017\* for all pollutants, to better characterize an average of a period without strike, as has been done in previous works (Silva et al., 2012). We used diurnal cycles since they make it easier to identify the hourly impact of vehicular emissions on air pollutants (Mayer, 1999).

Finally, statistical procedures were performed in order to quantitatively assess the influence of the truck strike on pollutant concentrations. Averages and standard deviations were calculated using all hourly measurements. Data distribution was calculated by violin plot graphs (Figs. 5–11) and histograms using Kernel Density Estimation (data not shown). Also, three significance tests were applied to the data ( $p < 0.05$ ) in order to check the influence of the strike on air pollution, that is, if there was a statistically significant difference between the averages of the period 2013–2017\* compared to 2018: the analysis of variance (ANOVA), the t-student test, and the Kruskal-Wallis test, which is more appropriate for non-parametric datasets such as air pollution data (Kalpasanov and Kurchatova, 1976). Our tested hypothesis was whether the averages of each air pollutant for the strike period was different from the average of the period without strike at each monitoring point.

### 3. Results and discussion

#### 3.1. Atmospheric analysis

The following analysis was carried out based on the synoptic charts presented in SM 4, and of Figs. 2 and 3. The year 2013 was characterized initially by a trough over the coast followed briefly by the Tropical then the Subtropical Atlantic High, bringing stability conditions which prevailed until the 27th of May. After the 28th, another approaching frontal system led to the development of pre-frontal, then, frontal conditions with southeast winds. These conditions are mostly favourable for higher pollutant concentrations during most of the period. During 2014, a frontal system reached the region between the 23rd and the 24th, bringing atmospheric instability, which prevailed until the 26th. From the 28th on, cold air from another frontal system on the coast influenced the MASP region, but the air becomes gradually drier and skies clearer,

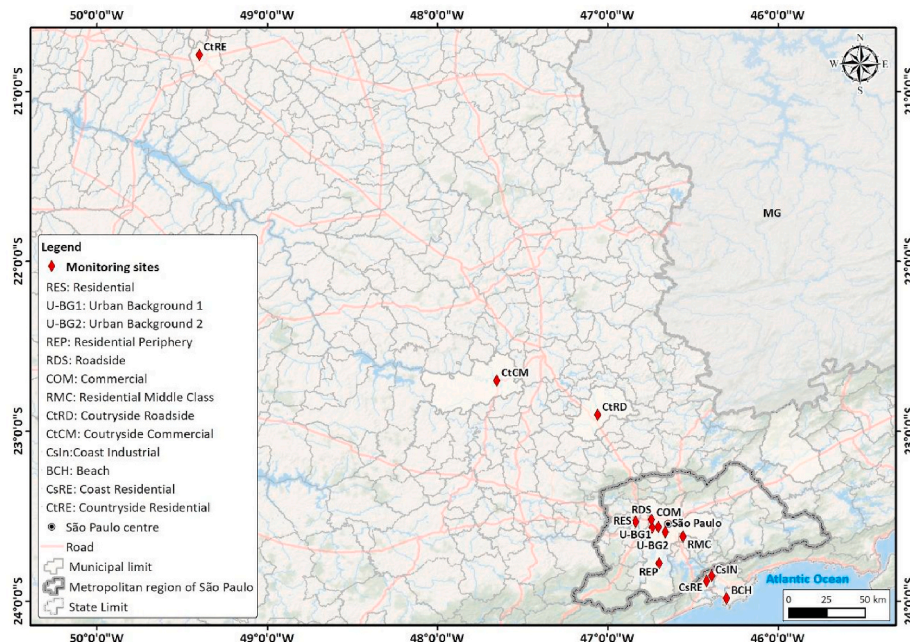


**Fig. 1.** Study area and monitoring sites used. Stations within the metropolitan region of São Paulo (RES, U-BG1, U-BG2, REP, RDS, COM, RMC) were chosen for analysis in the study. Stations located in the countryside (CtRD, CtCM, CtRE) and the coast (CsIN, CsRE, BCH) are briefly mentioned in the text and included in the supplementary material.

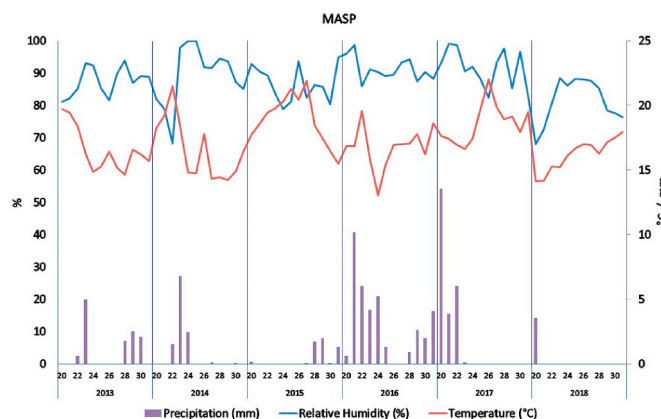


**Fig. 2.** Total precipitation and average air temperature and relative humidity for the period between May 20th to 31st in 2018 in the MASP.

as it brought polar air which was over the south of Brazil. This was the 2nd year with most rainy days the analysed period.

In 2015, a long stable and warm period prevailed with the influence of the Subtropical Atlantic High. Between the 28th and the 29th, a frontal system passes through the region, but the dry conditions return under the influence of the high-pressure extratropical air mass following the cold front. The year 2016 showed different conditions from the other years. The border of the Subtropical Atlantic High, located further out in the ocean, brought ocean humidity and precipitation to the MASP (differently of when its core is near the continent). On the 23rd, a frontal system passes through, bringing more instability and lower air temperatures. Unstable conditions prevail all through the period due to a trough in middle atmospheric levels east of the MASP and another frontal system reaching the region on the 30th.

The analysis for 2017 indicates frontal instability which brought rainy conditions for the beginning of the period until the 25th. However, the tropical Atlantic high prevails after that bringing higher air temperatures and drier air, unfavourable for the dispersion of pollutants. Finally, in 2018, the synoptic patterns are characterized by a frontal system in the beginning of the period with lower temperatures and precipitation in the 20th of May. However, the entire remainder of the period is influenced by the extratropical high-pressure air (1020 hPa), which brings stable and dry conditions, favourable for pollutant concentrations (Fig. 2). Atmospheric variables in the different years are shown in Fig. 2. Wind roses for the strike period in 2018 for a few selected sites show prevailing south-southeast and northwest winds,

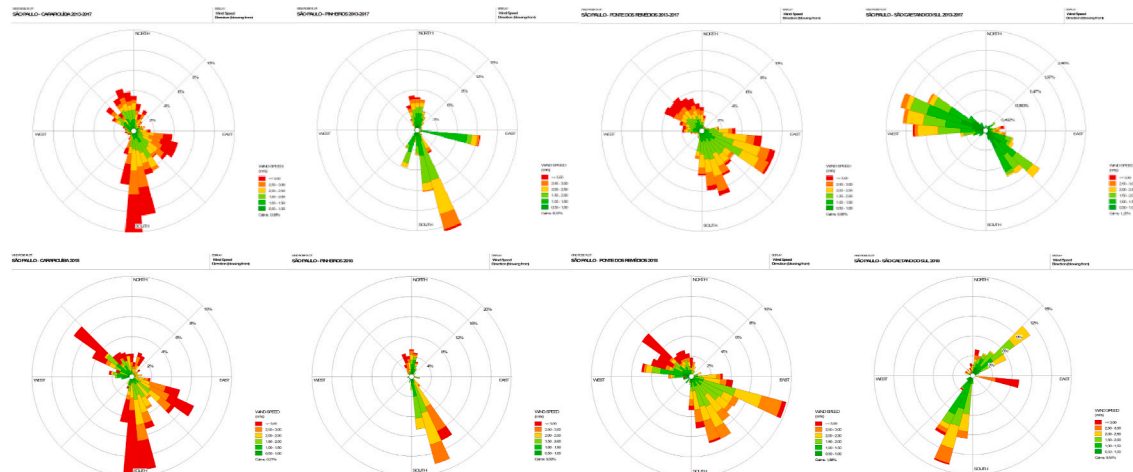
except for the RMC site, located to the east of the MASP (with southwest and northeast winds) (Fig. 3).

As observed by Sánchez-Ccoylo and de Fátima Andrade (2002), frontal systems are associated to lower pollutant concentrations in the MASP though upward motions and higher humidity, resulting in atmospheric instability. On the other hand, stable conditions with anti-cyclonic circulation were associated to higher pollutant concentrations, as has been observed by many studies in different regions (Liu et al., 2017). Thus, in order to compare the variations in air pollutants in different periods which are originated from emission changes, atmospheric patterns must be somewhat similar. In 2016 there is higher relative humidity and lower air temperature compared to previous years, also with many more rainy days, while in 2018, conditions are much more stable than in previous years, with higher temperature, lower humidity, and with the least amount of rainy days (Fig. 2). For this reason, we chose to discard the year 2016 from our analysis, since most of the analysed period in this year was influenced by frontal systems and overall atmospheric instability. It presented the highest percentage of rainy days (with precipitation > 0.1 mm) compared to other years (more than 80% of the days in the period). Comparing it to 2018, when more stable conditions prevailed, could lead to errors in detecting the role of emission changes brought about by the truck strike.

### 3.2. Satellite images

We show satellite images comparing the periods of strike with the period of regular activity. Since it was a national strike, we assumed the changes in pollutant concentrations could be observed on a regional scale by satellite images (Fig. 4–6).

For AOD (Fig. 4a), there is a decrease in 2018, which is of about 20% around the MASP but much higher in other regions, reaching 60% in the Atlantic Ocean and in other areas in the countryside. A study conducted in six Brazilian cities identified, as typical aerosol sources (besides vehicles), soil and crustal material, fuel oil combustion in industries, and land use change/biomass burning. Vehicles contribute to approximately 40% of total aerosol emissions in the MASP (Andrade et al., 2012; CETESB, 2018). Aerosol residence time in the atmosphere varies greatly, but it is typically of 3–7 days (Kristiansen et al., 2016). The decrease in AOD in the areas around the MASP could indicate the range to which the vehicular aerosol is transported inland or out to the sea due to the typical sea/land breeze local circulation in this region (Freitas et al., 2007; Chiquetto et al., 2018), which flows southeast/northwest. Data observed at countryside surface stations, however, indicate an increase in particulate concentrations, particularly for non-vehicular sites (supplementary material 2), which highlights the importance of different



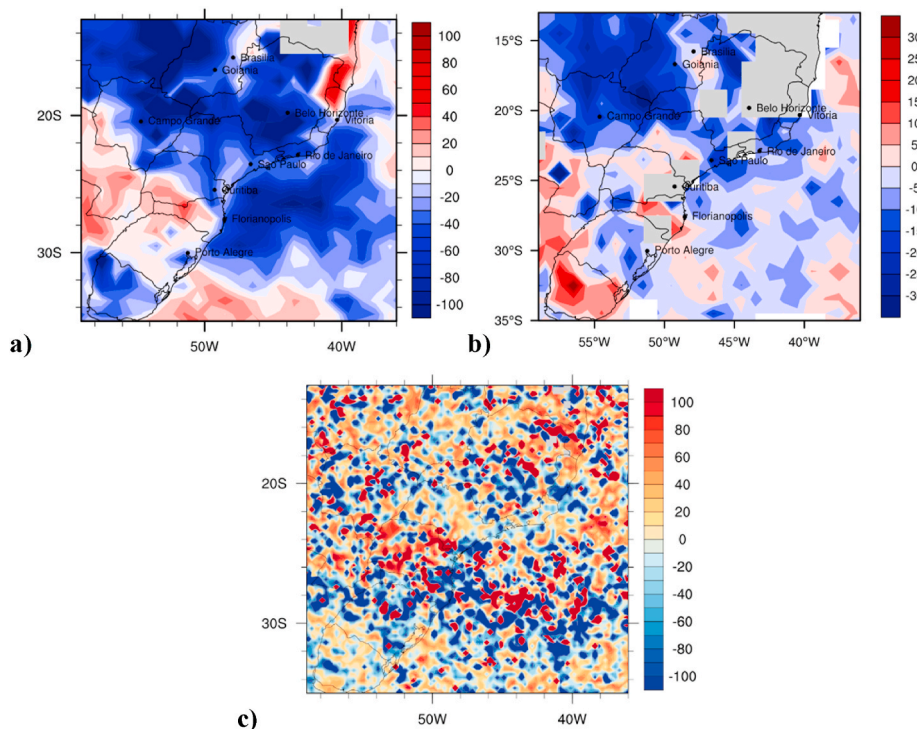


**Fig. 4.** (a, b, c): Difference in percentage for AOD (a), CO (b) and NO<sub>2</sub> (c) between the strike (average of 2018) and regular periods (average of 2013–2017\*). Sources: MODIS – Terra Satellite (AOD, [ladsweb.modaps.eosdis.nasa.gov/](https://ladsweb.modaps.eosdis.nasa.gov/)), MOPITT (CO (ppbv), grey areas indicate no valid data, <https://www2.acm.ucar.edu/mopitt>), OMI sensor – Aura Satellite (NO<sub>2</sub> (molecules cm<sup>-2</sup>), <https://giovanni.gsfc.nasa.gov/giovanni>)

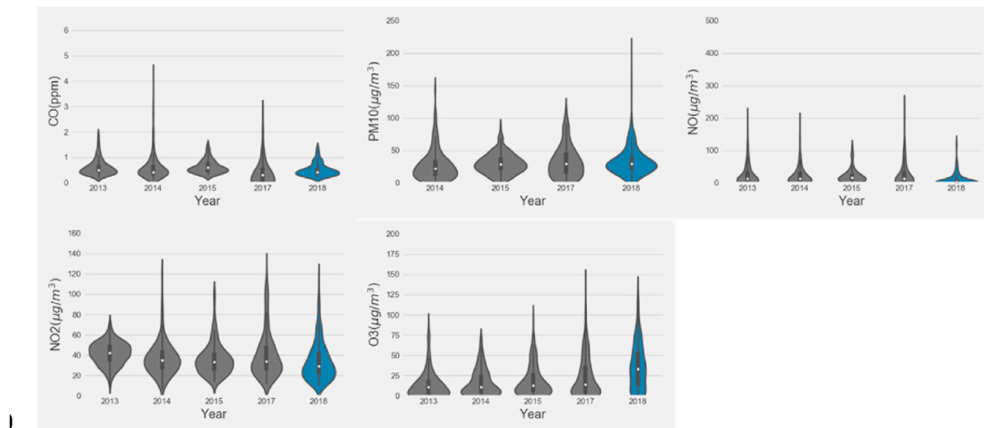


**Fig. 5.** Violin plots of criteria pollutants in the RES site in 2018 (blue) and in the previous years (2013–2017\*, grey). (For interpretation of the references to colour in this figure legend, the reader is referred to the Web version of this article.)

particulate sources such as biomass burning in the countryside of São Paulo. In 2018, the number of fires increased more than tenfold compared to the previous years, which will be addressed in the next section (Table 2).

The CO satellite image for the region shows a decrease in the areas around the MASP (Fig. 4b), of 15–20%. Main CO sources include burning of fossil fuels and biomass burning. About 97% of the CO in the MASP is emitted by automobiles (CETESB, 2018), but considering the whole Brazilian territory, it has been estimated that CO emission from industrial sources is equivalent or higher (Kawashima et al., 2020). As for the differences between strike and non-strike periods shown by satellite data, a similar phenomenon to AOD is observed: a decrease immediately over São Paulo and surrounding areas to the northwest and the Atlantic Ocean, possibly due to the decreased vehicle circulation on the coast. Areas with an increase in CO are also observed in many areas,

however, this might be influenced by biomass burning, particularly in the countryside west of São Paulo. There was not enough ground-based CO data for the countryside or the coast, with the exception of Campinas, also a large metropolitan area with 1.5 million people, where a decrease in CO was also observed (supplementary material 2). Ground-based CO observations in the MASP will be better discussed in the next section.

As for NO<sub>2</sub>, differences between the strike and regular periods do not follow the same pattern (Fig. 4c). There is no visually detectable spatial pattern over cities, although many areas in the countryside of the state experienced an increase. The aforementioned agricultural fires may have contributed to the increased NO<sub>2</sub> and particulate matter concentrations at the countryside, although NO concentrations in these regions also decreased during the strike (supplementary material 2). Directly over São Paulo, a slight increase in NO<sub>2</sub> during the strike period is

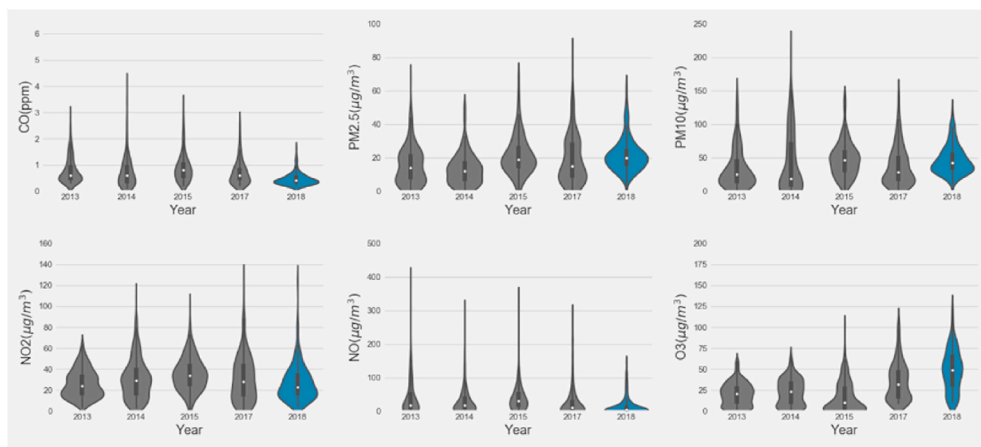


**Fig. 6.** Violin plots of criteria pollutants in the REP site in 2018 (blue) and in the previous years (2013–2017\*, grey). (For interpretation of the references to colour in this figure legend, the reader is referred to the Web version of this article.)

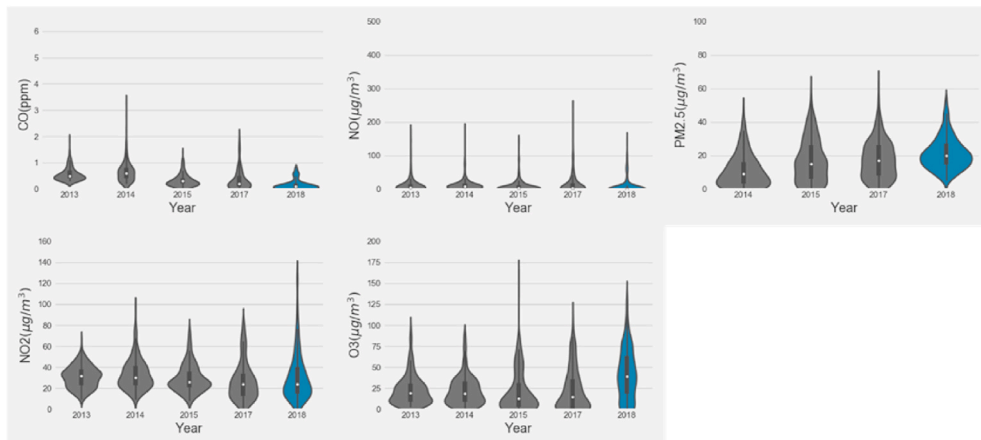


**Fig. 7.** Violin plots of criteria pollutants in the U-BG2 site in 2018 (blue) and in the previous years (2013–2017\*, grey). (For interpretation of the references to colour in this figure legend, the reader is referred to the Web version of this article.)

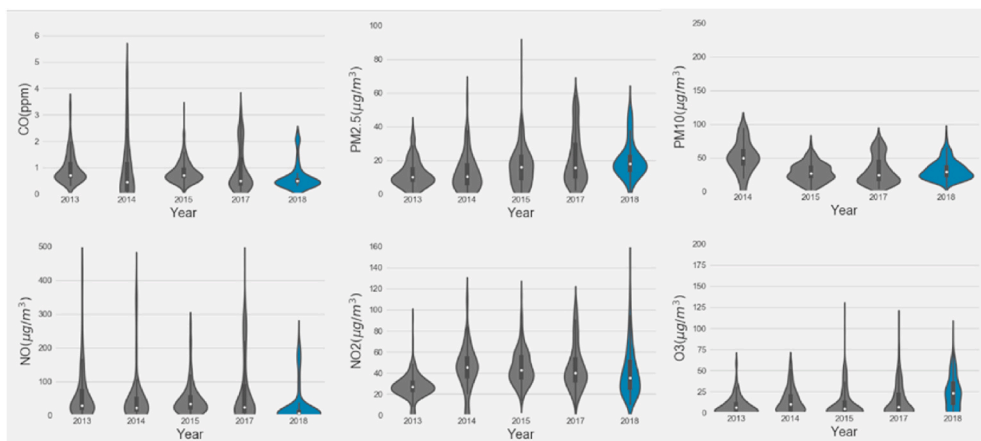


**Fig. 8.** Violin plots of criteria pollutants in the COM site in 2018 (blue) and in the previous years (2013–2017\*, grey). (For interpretation of the references to colour in this figure legend, the reader is referred to the Web version of this article.)

observed, compared to the regular periods, which highlights the importance of other sources, such as factories, biomass burning, and oxidation from NO by VOCs. At the coast, where industrial and vehicular sources prevail, and located away from the biomass burning regions in the countryside, both NO and NO<sub>2</sub> decreased, and there was a

statistically significant difference for all pollutants analysed (supplementary material 3). This also matches with the data observed at the ground-based stations presented in the next section.

## 2.2

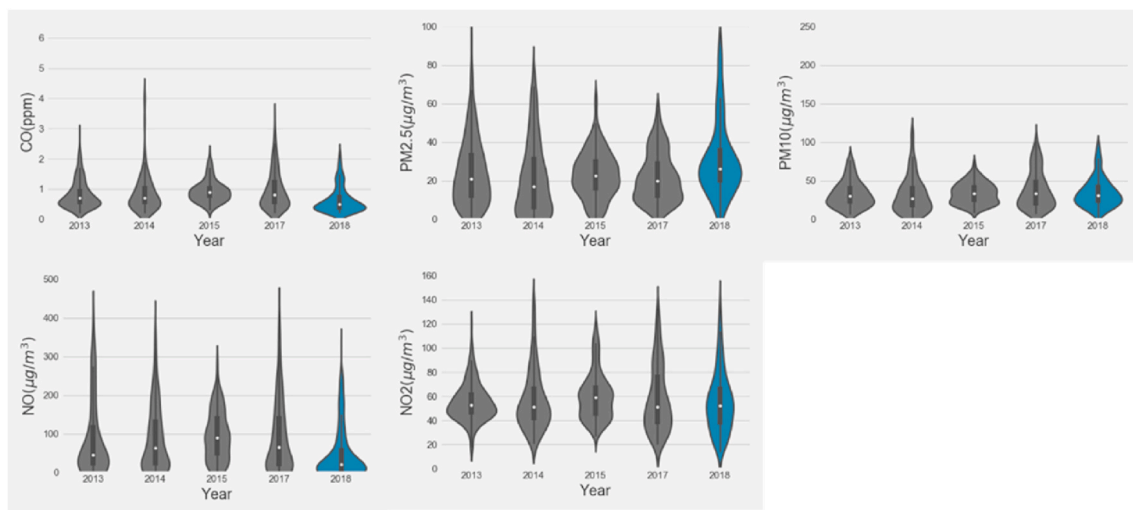


**Fig. 9.** Violin plots of criteria pollutants in the RDS site in 2018 (blue) and in the previous years (2013–2017\*, grey). (For interpretation of the references to colour in this figure legend, the reader is referred to the Web version of this article.)

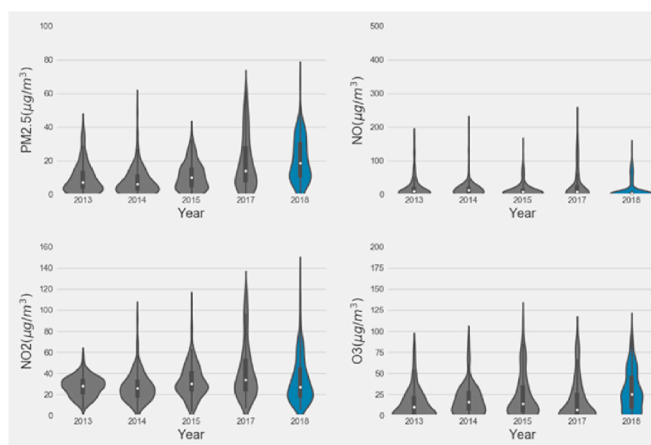


**Fig. 10.** Violin plots of criteria pollutants in the U-BG1 site in 2018 (blue) and in the previous years (2013–2017\*, grey). (For interpretation of the references to colour in this figure legend, the reader is referred to the Web version of this article.)

### 3.3. Statistics and hourly behaviour of pollutants during strike and regular periods

Results are shown by violin plots (Figs. 5–11), diurnal cycles (Figs. 12–17) and statistical tests (Table 4).

For CO, concentrations in 2018 were among the lowest in the periods analysed, both the averages and the distribution of data, particularly for the commercial (COM) and roadside (RDS) points (Figs. 8 and 9). The diurnal cycles reveal the strong influence of vehicular sources in the

**Table 1**

Average traffic count (km) for main avenues of São Paulo, for the period 21st–31st of May, comparing years without strike (2013–2017) and with strike (2018), using all hours of the day available.

Avenue	Total Traffic Count (km)	
	2013–2017	2018
Radial Leste	1975	1230
Washington Luís	2065	1415
Marginal Pinheiros	3528	2795
Marginal Tietê	4615	2670

Source: Traffic Engineering Company of the city of São Paulo (CET).

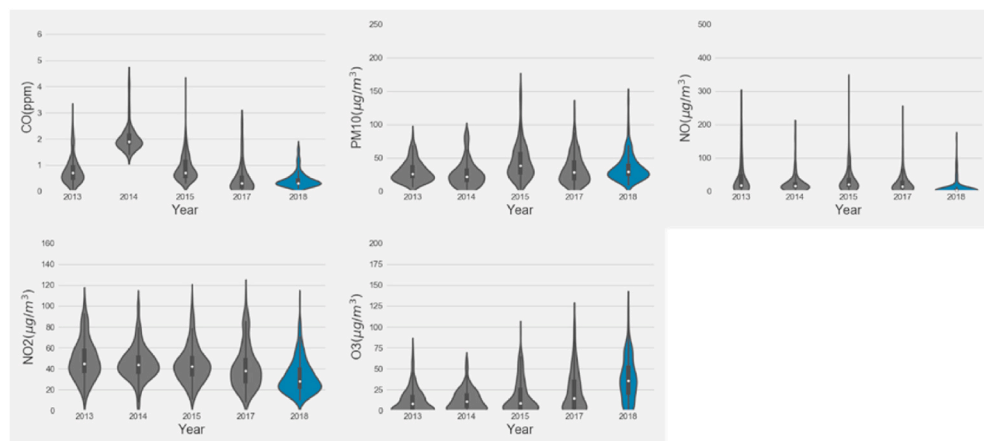


**Fig. 11.** Violin plots of criteria pollutants in the RMC site in 2018 (blue) and in the previous years (2013–2017\*, grey). (For interpretation of the references to colour in this figure legend, the reader is referred to the Web version of this article.)

**Table 2**

Number of fires in the state of São Paulo in the period 21st–31st of May.

Year	Number of fires
2013	580
2014	690
2015	495
2016	270
2017	230
2018	1675

Source: National Institute of Space Research (INPE), <http://queimadas.dgi.inpe.br/queimadas/bdqueimadas/>.

MASP, with morning and evening peaks associated with the rush hour, which is visible in all monitoring stations (Fig. 12). In the stations more directly under the influence of vehicles, such as RDS and COM, CO concentrations are higher, as well as in the residential middle class station (RMC), located in a small city in the MASP characterized by high income - in which there are 1.5 cars per person, the highest rate in Brazil. Moreover, the unusually high CO concentrations in 2014 could have been associated to local interferences and preparations for the 2014 World Cup (which took place in Brazil), such as a change in vehicle circulation in the MASP, or road maintenance/expansion works, combined with the already higher number of private vehicles in the vicinity of the RMC station. The lowest CO concentrations were registered in the Urban Background-1 (U-BG1) station, which is located far from vehicular emissions, and in the residential (RES) and residential urban periphery (REP) (characterized by lower income and less direct impact of private LDV).

Comparison between strike and non-strike periods show similar temporal profiles but with a marked decrease in CO concentrations during the strike (Fig. 12). The greatest difference was observed during the evening rush hour across all microenvironments. The RMC station, in which the maxima during 2013–2017\* was around 1.6 ppm at 19 h, decreased in more than 1 ppm, to 0.4 ppm, during the strike period. CO concentrations also show decreased variability (Figs. 5–11) which can also be associated with the decrease in overall vehicular activity, since CO is a typical tracer of primary vehicular emissions. Although it is emitted mostly by LDV, which originally were not involved in the mobilization, the truck strike interrupted the distribution of all fuel,

which impacted the circulation of LDV as well.

NO is also a primary pollutant, although it is emitted mainly by HDV and much more reactive than CO. NO concentrations also show two peaks, associated with urban traffic, and its highest peak occurs in the morning hours (Fig. 14). Among the studied sites, concentrations are also highest in the RDS and COM sites; followed by the residential areas (RES, RMC, REP), and lowest at the U-BG2 site. Naturally, the impacts of the truck strike are more intense at the RDS site (at 20 h, the average concentration dropped from 90 to 10  $\mu\text{g m}^{-3}$ ). At the RES and urban background stations (U-BG1, U-BG2), the impacts of the strike are less evident, although decreases were also observed, reaching nearly zero during the afternoons (perhaps suggesting that most of NO was converted to  $\text{NO}_2$  in the mornings). The violin plots show that the total NO averages in 2018 at these locations were close to zero, in spite of its high variability (Figs. 5–11).

The impact of the 2018 strike, however, was mixed for  $\text{NO}_2$  among the sites. Most sites show lower concentrations in 2018 (indicated by the

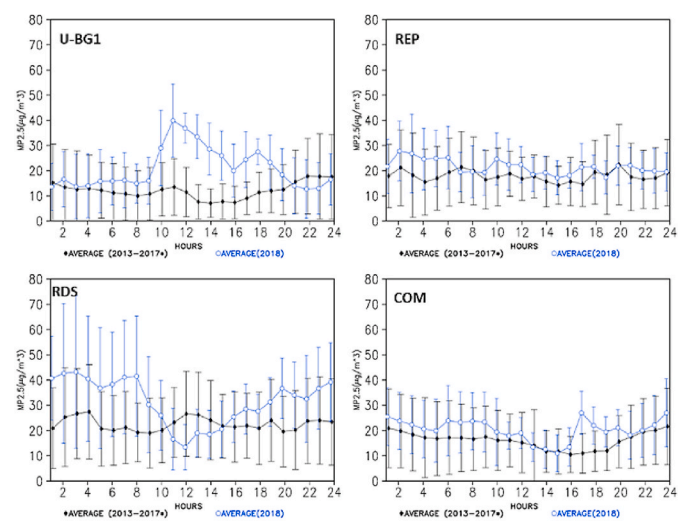


Fig. 13. Diurnal cycles of  $\text{PM}_{2.5}$  during the strike (blue) and non-strike periods (black). (For interpretation of the references to colour in this figure legend, the reader is referred to the Web version of this article.)

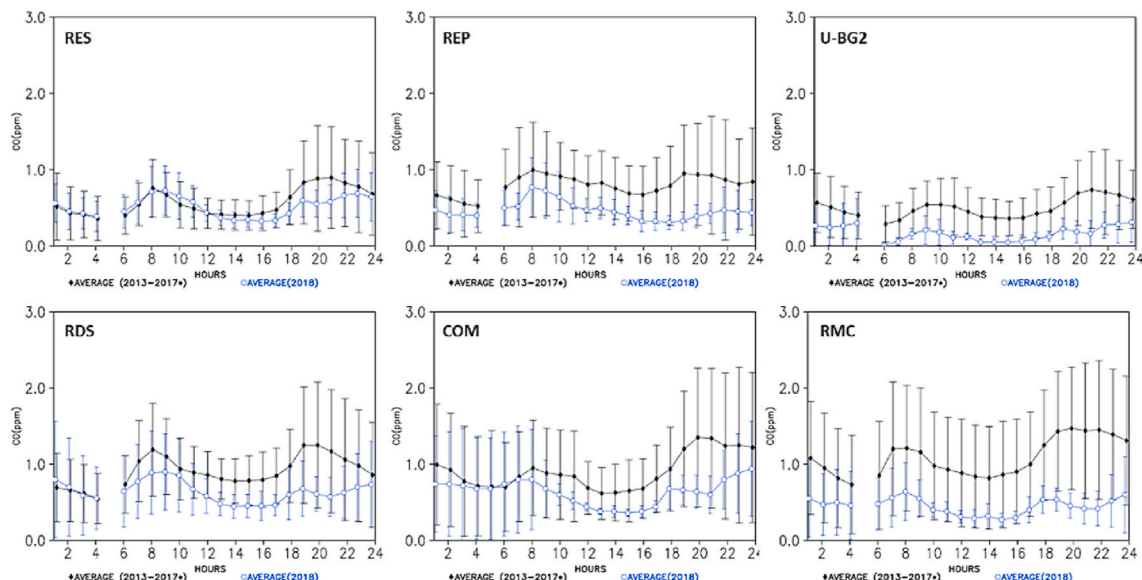
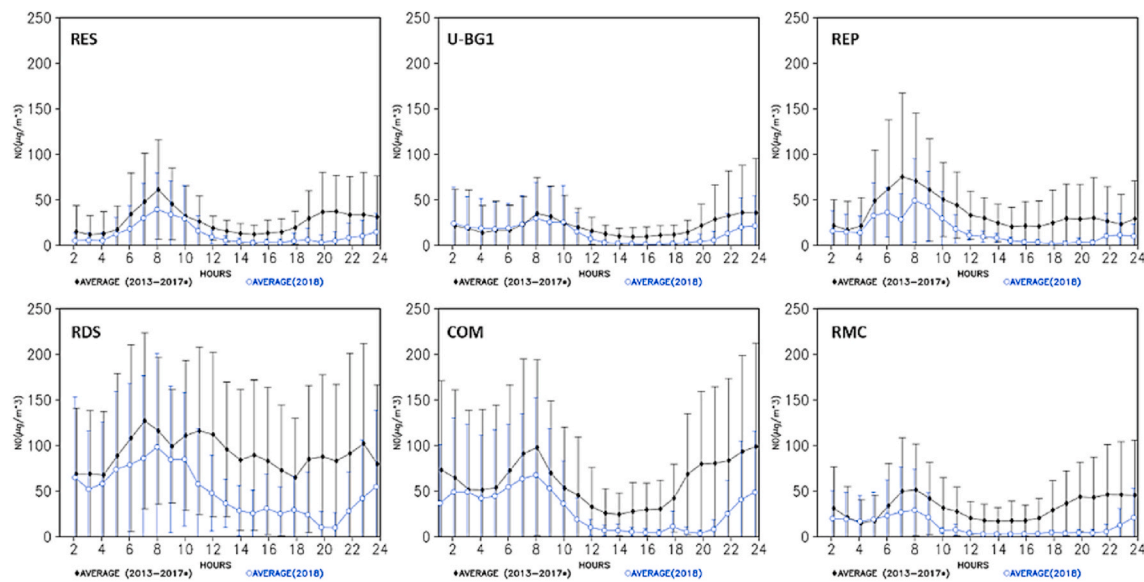
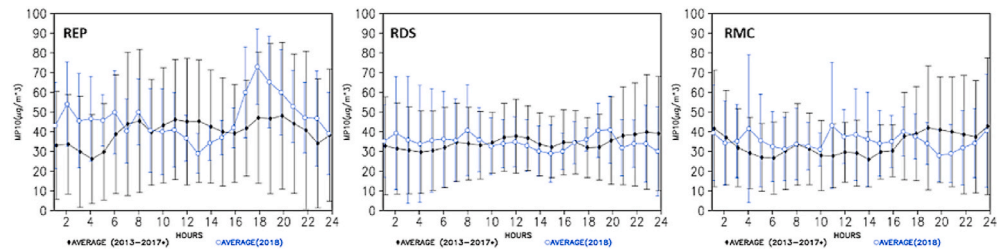


Fig. 12. Diurnal cycles of CO during the strike (blue) and non-strike periods (black). (For interpretation of the references to colour in this figure legend, the reader is referred to the Web version of this article.)



**Fig. 14.** Diurnal cycles of NO during the strike (blue) and non-strike periods (black). (For interpretation of the references to colour in this figure legend, the reader is referred to the Web version of this article.)



**Fig. 15.** Diurnal cycles of PM<sub>10</sub> during the strike (blue) and non-strike periods (black). (For interpretation of the references to colour in this figure legend, the reader is referred to the Web version of this article.)

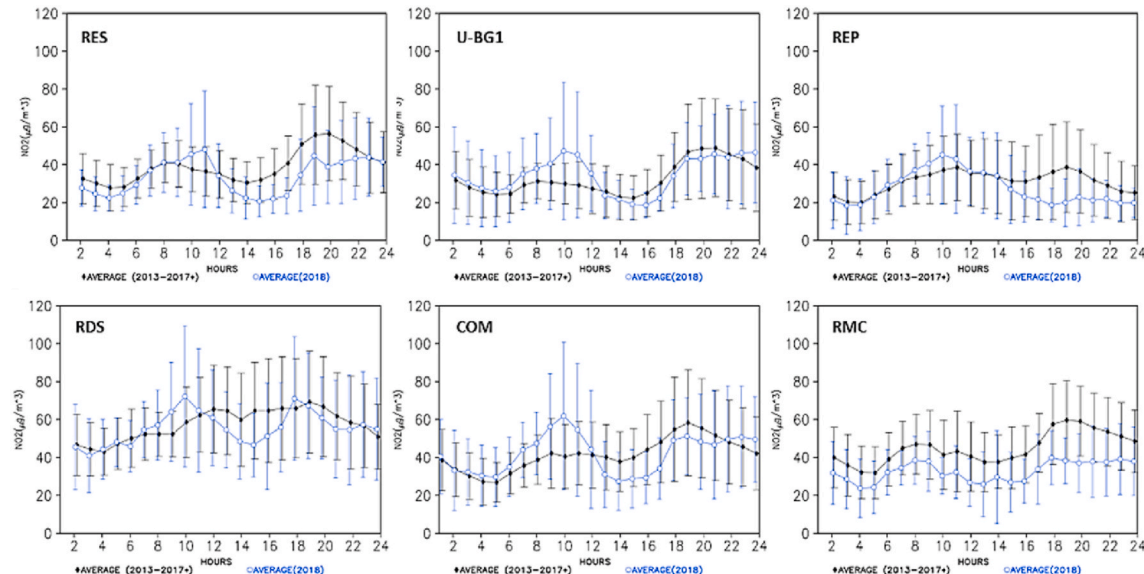


**Fig. 16.** Diurnal cycles of NO<sub>2</sub> during the strike (blue line, 2018) and non-strike periods (black line, 2013–2017\*). (For interpretation of the references to colour in this figure legend, the reader is referred to the Web version of this article.)

pear-shaped violin plots, Figs. 5–11). The diurnal cycles show that the NO<sub>2</sub> decrease in 2018 was not proportional among the hours of the day, occurring from 12 h to the early morning hours (Fig. 16). However,

during the morning, NO<sub>2</sub> concentrations in 2018 actually increased at most observed sites. NO<sub>2</sub> concentrations were higher at the same sites in which CO was higher: RDS, COM and RMC, with lower concentrations at

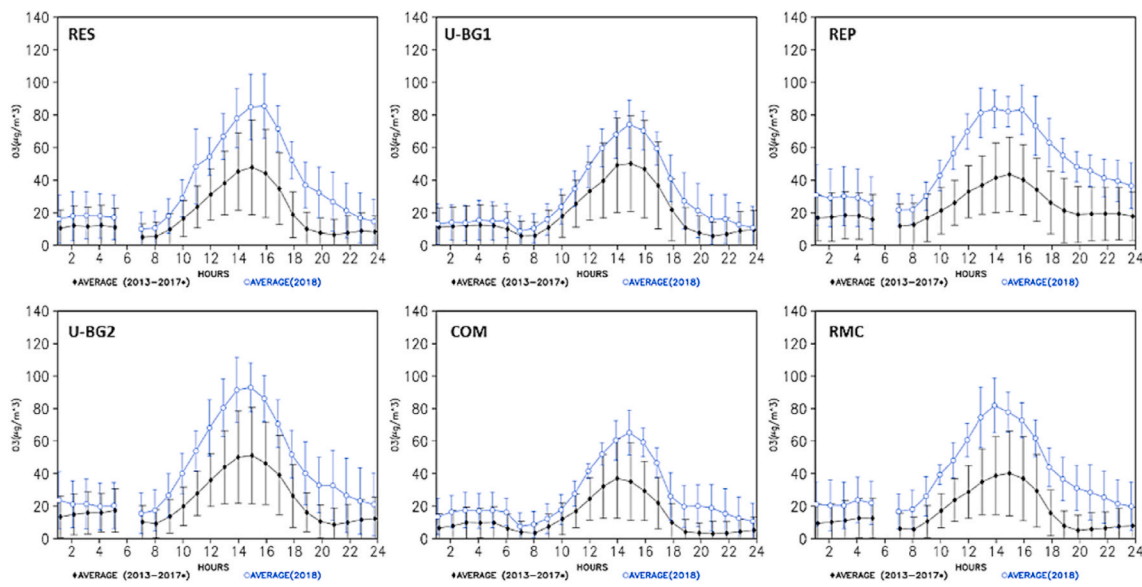


**Fig. 17.** Diurnal cycles of  $O_3$  during the strike (blue line, 2018) and non-strike periods (black line, 2013–2017\*). (For interpretation of the references to colour in this figure legend, the reader is referred to the Web version of this article.)

the RES and the U-BG2 (Figs. 5–11). During 2013–2017\*, concentrations remained high at the RDS site during most of the day due to the continuous influence of HDV. At the REP site (Fig. 16), this can also be observed (although to a lesser extent), probably due to the influence of the *Rodoanel* (a motorway ring around São Paulo designed to decrease the truck traffic inside the urban centre), located at approximately 500 m to the south. At the other sites, vehicular influence is perceived similarly to CO and NO, with the rush hour peaks in the morning and evening, and lower concentrations during the day.

The high availability of sunlight in 2018 could have photolyzed most  $NO_2$  into  $NO + O$  during the afternoons, which would explain the decrease in  $NO_2$  after midday (possibly linked to the increase in  $O_3$ ). An exception was the RMC site, where  $NO_2$  remained lower in 2018 during the entire day and showed the greatest decrease, from 62 to 35  $\mu g m^{-3}$  ( $-27 \mu g m^{-3}$ ). Due to its more eastern position compared to the other sites, it could have been affected by the sea breeze which favours pollutant transport and dispersion (Bischoff-Gauß et al., 1998; Chiquetto et al., 2018), which is shown by wind direction in Figure 3. At other eastern sites, near the coast,  $NO_2$  concentrations were also lower during the entire day in 2018, although they are heavily impacted by industry (supplementary material 2). Anyway, the increase in the morning  $NO_2$  during 2018 in most sites could be linked to either atmospheric conditions more favourable for higher concentration of pollutants in 2018, or the importance of other emission sources, such as fires. In fact,  $NO_2$  and particulate matter experienced unexpected increases in 2018, which could be linked to the much higher number of fires in the countryside of São Paulo in 2018 (Table 2). However,  $NO_2$  usually remains only one day in the atmosphere before being removed, so there is limited time for atmospheric transport as compared to particulate matter. Overall, the impacts of strike on  $NO_2$  are more complex than on entirely primary pollutants, as showed by recent studies which investigated pollutant emission changes during the lockdown due to the COVID-19 pandemic (Nakada and Urban, 2020; Kanniah et al., 2020; Muhammad et al., 2020; NASA, 2020).

For the particulate matter, no discernible impact of the strike could be observed in the diurnal cycles (Figs. 13 and 15), or in the violin plots (Figs. 5–11). Concentrations during the strike period remained in similar levels of the previous years, or even higher. At the RDS site, a sharp decrease in  $PM_{2.5}$  is observed from 8 to 20 h but remaining much higher through the night than in the average of previous years (Fig. 13). A similar behaviour is observed for  $PM_{10}$  (Fig. 15) at this site, and for

$PM_{2.5}$  at the COM site. Since these are the sites with the most direct influence of vehicular emissions, we theorize that such decreases could be associated with the truck strike, particularly  $PM_{2.5}$  which is more strongly linked to combustion. On the other hand, a sharp increase is noted in the U-BG2 site during the same period of the day. At the remaining sites, no visually discernible trend is perceived. This seemingly contradicts AOD observations (Fig. 4), which indicate an average decrease, but other studies have also showed discrepancies between satellite AOD data and ground-based PM, particularly due to changes in vertical mixing during clear-sky samplings, as observed in winter over the western US (Li et al., 2015).

Particulate matter has a rather broad range of sources in the atmosphere other than vehicles, such as industrial activity, biomass burning, soil resuspension, sea salt, and, of course, secondary particulate formation in the atmosphere. For the MASP, the São Paulo State Environmental Agency estimates the following relative contribution to the particulate matter: vehicles 40%, industrial activity 10%, 25% soil resuspension and 25% secondary particulate formation (although there is high uncertainty and it could be as high as 50%) (CETESB, 2018). But more studies are needed for a better assessment, as for example, recent studies showed that the emission of pizzerias in São Paulo can be important sources of particles (Lima et al., 2019) and that secondary formation processes account for about 43% of PM1 particles (Brito et al., 2018). The massive absence of vehicles did not seem to impact much the concentrations during the strike period, which highlights the importance of the non-vehicular PM sources, the influence of atmospheric conditions including possible atmospheric transport from nearby regions, as well as secondary reactions in the atmosphere. In fact, a combination of one or more of these factors has been suggested for the observed increase in PM concentrations in a recent study during the COVID-19 lockdown in China (Le Quéré et al., 2020). A study during a strike period in Spain also showed similar results (Basagaña et al., 2018).

The study period coincides with the season of sugar cane burning (before the harvest) in the countryside of the São Paulo state, when there are usually a large number of fires (Paraiso and Gouveia, 2015). The state of São Paulo experienced a much greater number of fires in 2018 than in the previous years analysed (2013–2017), which could be associated to the high concentrations of particulate material in 2018 in spite of the decrease in vehicular emissions, which is in fact observed in the countryside monitoring stations (Supplementary material 1 and 2).

In fact, some studies have demonstrated this phenomenon in Brazil

and in São Paulo (Pereira et al., 2011, 2017). This hypothesis can be further reinforced due to the decrease in particulate matter observed during the strike in industrial sites located at the coast, in the city of Cubatão (supplementary material 1 [1.3, 1.4], and SM2 [2.2 and 2.4], sites CsIn and CsRe), infamous for its historically high air pollution levels (Vieira-Filho et al., 2015). Located near the coast, its greater distance from the agricultural areas in the countryside, coupled with the presence of mountain ranges such as Serra do Mar (which could have acted as geographical barriers) might have played a role in the decrease in PM observed in 2018 in these areas, by preventing the transport of particles from the intense biomass burning events observed in 2018 in countryside areas in the state of São Paulo. However, more specific analyses such as backward trajectory studies and PM chemical composition analyses, would be required to confirm this.

Ozone concentrations experienced an increase during 2018 at all sites, both in average values and also in its variability (Fig. 17 and Figs. 5–11). Concentrations were higher at the U-BG and the REP sites, which are located further away from emissions, and lowest at the RMC (there is no O<sub>3</sub> measurements at the RDS site). Concentrations reach a peak in the afternoon when sunlight availability and concentration of precursors are higher. This shows that the impact of vehicular sources on secondary pollutants is complex and considerably different than on primary pollutants. Ozone is involved in non-linear atmospheric chemistry processes of formation and consumption, in which its concentrations are highly dependent on the availability of sunlight and on the NO<sub>x</sub>/VOCs ratio. Although we do not have any VOC data, NO<sub>x</sub> emissions certainly decreased, as well as some of its concentrations (Figs. 14 and 16), which could have changed the NO<sub>x</sub>/VOCs ratio. Considering that São Paulo is a NO<sub>x</sub>-saturated environment (Alvim et al., 2018), there is a relative abundance of NO<sub>x</sub>, and so, ozone formation will depend on the concentration of VOCs. A decrease in VOCs leads to a decrease in ozone, but a decrease in NO<sub>x</sub> might lead to an increase in ozone (Orlando et al., 2010; Chiquetto et al., 2016; Alvim et al., 2018). So, this decrease in NO<sub>x</sub>, along with a great availability of sunlight and stable conditions in 2018 (Fig. 3), probably played a role in the increase in ozone observed in 2018. The maximum increase in O<sub>3</sub>, of about 40 µg m<sup>-3</sup>, occurred at the U-BG1 and the REP sites, with an average increase of 10–15 µg m<sup>-3</sup> in most sites.

From this set of results, it is clear that the truck strike impacted primary and secondary air pollutants in different ways, at the different microenvironments analysed. Absolute hourly maximums during the strike were also compared to the periods without strike in Table 3. A decrease was observed for all monitored pollutants during the strike, particularly for CO (−67%) and NO (−47%). NO<sub>2</sub> and ozone showed the smallest decreases. As noted in the other analyses, NO and CO did not increase during the strike, but particulate matter, NO<sub>2</sub> and ozone showed increases in the hourly maximums during the strike period, particularly PM<sub>10</sub> (+41%), which agrees with other results shown here.

Statistical tests results, confirming these differences, are presented in

Table 3

Decreases and increases in the maximum hourly concentrations in the non-strike and strike periods (in blue). N/A means no increase during the strike.

Pollutant	Hourly maximum (decreased during strike)	Station	Hourly maximum (increased during strike)	Station
CO (ppm)	4.3/1.4 (−67%)	RES	N/A	N/A
PM <sub>2.5</sub> (ug·µ <sup>-3</sup> )	84/57 (−33%)	COM	63/70 (+10%)	U-BG1
PM <sub>10</sub> (ug·µ <sup>-3</sup> )	203/123 (−39%)	REP	146/206 (+41%)	RES
NO (ug·µ <sup>-3</sup> )	457/243 (−47%)	COM	N/A	N/A
NO <sub>2</sub> (ug·µ <sup>-3</sup> )	111/104 (−7%)	RMC	116/151 (+31%)	COM
O <sub>3</sub> (ug·µ <sup>-3</sup> )	161/135 (−16%)	U-BG2	108/122 (+13%)	REP

Table 4

Kruskal-Wallis test between strike and non-strike periods. Bold means a statistically significant difference; asterisks indicate no statistical significance; N/A indicates data not available.

Site/Pollutant	CO	NO	NO <sub>2</sub>	PM <sub>10</sub>	PM <sub>2.5</sub>	O <sub>3</sub>
Residential (RES)	0.09*	0.00	0.00	0.00	N/A	0.00
Urban Background 1 (U-BG1)	N/A	0.00	0.80*	N/A	<b>0.00</b>	0.00
Urban Background 2 (U-BG2)	0.00	0.00	0.01	N/A	0.00	0.00
Residential Periphery (REP)	0.00	0.00	0.00	0.00	0.00	0.00
Roadside (RDS)	0.00	0.00	0.10*	0.46*	0.00	N/A
Commercial (COM)	0.00	0.00	0.12*	0.12*	0.00	N/A
Residential Middle Class (RMC)	0.00	0.00	0.00	0.03	N/A	0.00

**Table 4.** The Kruskal-Wallis, ANOVA and T-Student tests were performed. However, the T-Student did not present as much statistical differences among the pollutants compared to the ANOVA and the Kruskal-Wallis test. This is probably due to the fact that it is more suited for parametric datasets (which usually is not the case with air pollutants). Results from the Kruskal-Wallis test (Table 4) revealed similar patterns to those observed by the diurnal cycles; ANOVA yielded similar results, which reinforced our conclusions (data is not shown).

NO<sub>2</sub> and PM<sub>10</sub> showed the least statistical difference between the strike and non-strike periods, mostly at sites under a greater impact of vehicular emissions such as RDS and COM, while for O<sub>3</sub>, NO and PM<sub>2.5</sub>, the difference was significant for all sites. PM<sub>2.5</sub> concentrations were actually higher during the strike period (Fig. 13), which could be the influence of different sources, as discussed previously, and should be investigated using other tools and approaches. Similar results for PM<sub>10</sub> were obtained at the countryside (supplementary material 3), where the RDS station did not show significant difference for PM<sub>10</sub> between strike and non-strike periods, while residential (RES, RMC, REP) and the COM locations did, and it also was higher in 2018 (Supplementary material 1 and 2). For CO, all sites showed a statistically significant difference except for the RES, which is actually visible in Fig. 12. These results reinforce that the impact of the strike was clearer for primary (NO and CO – decrease) and secondary pollutants (O<sub>3</sub> – increase), while for pollutants with a mix of sources and composed of primary and secondary fractions (PM<sub>10</sub>, PM<sub>2.5</sub>, NO<sub>2</sub>), impacts varied according to the micro-environment analysed.

Comparing these conclusions to other studies, similar results can be observed. Concerning CO, an average decrease of more than 50% was perceived for the U-BG1 and the commercial (COM) sites (Figs. 5–11), which was comparable to that observed during a nationwide truck strike in India (Sharma et al., 2010). Another public strike study in the India (for Hyderabad) also showed significant reduction in CO (20%), although there was a decrease in BC (48%) and PM (28%) (Mahalakshmi et al., 2014), which was not perceived in this study for the MASP. In fact, many studies observed that decreases in particulate matter are different and not as linear compared to primary pollutants, which has to do with its diversity of sources and processes, including secondary particle formation (Basagaña et al., 2018; Leirão et al., 2020). Concerning ozone, other works about changes in vehicular emission also show an increase in its concentrations during these periods, usually in downtown locations but not restricted to them, and of course, given that meteorological conditions were favourable (Meinardi et al., 2008; Levy, 2013).

The changes in emissions brought about by massive transport sector strikes, national holidays or aggressive restriction policies, can be compared, to a degree, to those related to the lockdown and interruption of activities due to the COVID-19 pandemic. Ever since the World Health Organization declared COVID-19 as a global pandemic, decreases in pollutant emissions have been observed in many locations around the globe (Le Quéré et al., 2020; Chen et al., 2020; ESA, 2020a; ESA, 2020b). Since social isolation became one of the main preventive measures

against the spread of the COVID-19 contamination, vehicle activity has decreased in unprecedented ways, leading to an expressive drop in vehicular emissions worldwide. Similarly to the truck strike evaluated in this study, CO and NO levels showed greater decrease in South Asia, China and in Brazil in lockdown periods, while for NO<sub>2</sub> the decrease was not as strong due to emissions related to industrial activity (Le Quéré et al., 2020; Global Energy Review 2020; Nakada and Urban, 2020; Kanniah et al., 2020; Siciliano et al., 2020; ESA SEC, 2020; NASA, 2020; Muhammad et al., 2020). Nakada and Urban (2020) also showed how impacts for PM were more complex than for CO and NO during the partial lockdown in April 2020. However, other studies showed that average PM<sub>2.5</sub> concentration levels decreased in the pandemic, although it varied according to the location studied (ESA, 2020a; CAMS, 2020; Wu et al., 2020; Zambrano-Monserrate et al., 2020). Meanwhile, PM<sub>10</sub> showed a different pattern and decreased only in certain periods in regions in Brazil, India and Spain (Nakada and Urban, 2020; Sharma et al., 2020; Zambrano-Monserrate et al., 2020; Tobías et al., 2020). Ozone, on the other hand, increased all locations analysed, by almost 30% (Siciliano et al., 2020; Mahato et al., 2020; Nakada and Urban, 2020; Tobías et al., 2020). It is clear that these results mostly agree with the findings of our study, which indicate that the impacts of the vehicular fleet are much more easily perceivable for primary reactive pollutants. Other regional pollution sources, such as fires and factories, must be taken into consideration for the analysis of NO<sub>2</sub> and PM, while the high ozone concentrations also remain a challenge for policymakers, due to its increases even when vehicular emissions are greatly decreased, at least, for a relatively short period of time.

#### 4. Conclusions

We analysed the impact of a truck drivers' strike on air pollution in the Metropolitan Area of São Paulo (MASP), which took place in 2018, from May 21st to 31st. We compared CO, NO, NO<sub>2</sub>, PM<sub>10</sub>, PM<sub>2.5</sub> and O<sub>3</sub> hourly data from this period with the same period from previous years. We briefly analysed the atmospheric conditions (which led to the exclusion of 2016 from the analysis), and used satellite images, diurnal cycles and statistical tools to represent the differences. The truck driver's strike restrained not only the circulation of trucks, but of light-duty vehicles (due to the shortages in fuel supply by trucks) and buses (of which the fleet was reduced by 30–60%), so different impacts were observed on air pollution in the MASP.

Primary pollutants directly associated with vehicular emissions, such as CO and NO, decreased sharply in 2018 during all hours of the day. Statistically significant differences between periods with and without strike were observed in nearly all sites analysed for these pollutants. NO decreased to nearly zero in the afternoon during the strike, and CO concentrations decreased by 50%. For NO<sub>2</sub>, the impacts of the strike were not as marked and not as statistically significant, particularly at sites under more intense vehicular emissions. Most sites showed higher NO<sub>2</sub> concentrations in the morning but lower NO<sub>2</sub> in the afternoon during the strike period, possibly due to increased photolysis, favoured by the clear conditions observed in 2018. For particulate matter, mixed results were observed, although PM<sub>2.5</sub> concentrations increased in all sites in 2018 compared to the previous years, showing that the impacts of the strike for pollutants with an important secondary fraction were different from primary pollutants, and even from entirely secondary pollutants such as O<sub>3</sub>. In fact, O<sub>3</sub> concentrations increased in all monitoring sites, particularly during the afternoon and at sites located farther from the roads (with an average hourly maximum increase of 40 µg m<sup>-3</sup>, or 50%). We theorize that this could be due to atmospheric conditions favourable for its formation (dry and sunny), along with the decrease of NO<sub>x</sub> in a NO<sub>x</sub>-saturated environment such as the MASP.

These results show that the MASP is under considerable influence of vehicular emissions, although the impacts varied among pollutants. Primary (NO, CO) and secondary (O<sub>3</sub>) pollutants showed statistically significant differences during the strike period, while impacts for

pollutants with both primary and secondary fractions were mixed (NO<sub>2</sub>, PM<sub>10</sub> and PM<sub>2.5</sub>). Clearly, technological improvements in engine, maintenance and fuel quality of all vehicle types are necessary to decrease primary emissions. But these results highlight the importance of (1) atmospheric conditions, (2) the secondary formation of pollutants in the atmosphere, (3) the regional non-vehicular pollution sources and (4) possible pollutant transport (ex: from nearby areas due to the unusually high number of fires in 2018), which affect the concentrations of pollutants in a complex urban area such as the MASP. If decreases in PM or O<sub>3</sub> are to be attained, integrated policies which regulate PM, NO<sub>x</sub> and particularly VOCs emissions, also from other sectors, such as industry and agribusiness, should be implemented.

Particularly at this moment, when the pandemic situation imposes severe restrictions in vehicle use, policymakers must implement mobility strategies focused on improving active and micromobility use, including bicycles, walking, etc. Also, realistic approaches are needed for developing countries, such as in areas like the periphery of the MASP. Low-income population, highly dependent on crowded public transport systems, could benefit immensely from decreasing distances between housing and available jobs. Coupled with the technological improvements, such measures would help not only to mitigate total vehicular emissions but also to improve quality of life while ensuring social distancing during the daily commute. Since air pollution impacts from studies performed during the lockdown period are similar to our findings from the strike period, this study can be considered a proxy for future lockdown situations brought by a possible second wave of COVID-19, and also by entirely new pandemics, revealing the new air quality challenges to be addressed in the future. In this context, a properly integrated urban management considering all sectors, such as health, energy, transport and the environment, is key for an improved governance aiming towards more environmentally-resilient megacities in the future.

#### CRediT authorship contribution statement

**Júlio Barboza Chiquetto:** Conceptualization, Writing - original draft, Writing - review & editing, Supervision. **Débora Souza Alvim:** Methodology, Resources, Software. **José Roberto Rozante:** Formal analysis, Investigation. **Marlon Faria:** Formal analysis, Methodology, Data curation. **Vinícius Rozante:** Visualization. **João Paulo Assis Gobo:** Investigation, Project administration, Writing - review & editing.

#### Declaration of competing interest

The authors declare that they have no known competing financial interests or personal relationships that could have appeared to influence the work reported in this paper.

#### Acknowledgements

To Gabriela Rozante, who provided help with the graphical abstract, and Lady Silveira, who gently provided us with Fig. 1 (map).

#### Appendix A. Supplementary data

Supplementary data to this article can be found online at <https://doi.org/10.1016/j.atmosenv.2020.118072>.

#### References

Alvim, D.S., Gatti, L.V., Corrêa, S.M., Chiquetto, J.B., Santos, G.M., de Souza Rossatti, C., Pretto, A., Rozante, J.R., Figueroa, S.N., Pendharkar, J., Nobre, P., 2018. Determining VOCs reactivity for ozone forming potential in the megacity of São Paulo. *Aerosol Air Qual. Res.* 18, 2460–2474. <https://doi.org/10.4209/aaqr.2017.10.0361>.

Andrade, M. de F., de Miranda, R.M., Fornaro, A., Kerr, A., Oyama, B., de Andre, P.A., Saldiva, P., 2012. Vehicle emissions and PM<sub>2.5</sub> mass concentrations in six Brazilian

cities. *Air Qual. Atmosphere Health* 5, 79–88. <https://doi.org/10.1007/s11869-010-0104-5>.

Basagaña, X., Triguero-Mas, M., Agis, D., Pérez, N., Reche, C., Alastuey, A., Querol, X., 2018. Effect of public transport strikes on air pollution levels in Barcelona (Spain). *Sci. Total Environ.* 610–611, 1076–1082. <https://doi.org/10.1016/j.scitotenv.2017.07.263>.

Bischoff-Gaib, I., Kalthoff, N., Fiedler, F., 1998. The impact of secondary flow systems on air pollution in the area of São Paulo. *J. Appl. Meteorol.* 37, 269–287. <https://doi.org/10.1175/1520-0450-37.3.269>.

AMS, <https://atmosphere.copernicus.eu/amid-coronavirus-outbreak-copernicus-monitors-reduction-particulate-matter-pm25-over-china> (accessed on 18 June 2020).

CGE. São Paulo municipal emergency management centre. Available at: <https://www.cgesp.org/v3/estacoes-meteorologicas.jsp>. Accessed on 21 November 2019.

Brito, Joel, Carbone, Samara, Santos, Djacinto A. Monteiro dos, Dominutti, Pamela, Alves, Nilmar de Oliveira, Rizzo, Luciana V., Artaxo, Paulo, 2018. Disentangling vehicular emission impact on urban air pollution using ethanol as a tracer, 8(1), pp.1-10. *Nature Scientific Reports* 8 (10679), 1–10. <https://doi.org/10.1038/s41598-018-29138-7>. In this issue.

CETESB, 2018. *Air Quality Report for the São Paulo State 2017*. Environmental Agency of the State of São Paulo.

Chiquetto, J.B., Ribeiro, F.N.D., Alvim, D.S., Ynoue, R.Y., Silva, J.D., Silva, M.E.S., 2018. Transport of pollutants by the sea breeze in São Paulo under the south atlantic high. *Geogr. Dep. Univ. São Paulo* 148–161. <https://doi.org/10.11606/rdg.v0ispe.143050>.

Chiquetto, J.B., Ynoue, R.Y., Miranda, W.C., Silva, M.E.S., 2016. Concentrações de ozônio troposférico na Região Metropolitana de São Paulo e a implementação de parques urbanos: observações e modelagem. *Boletim Paul. Geogr.* 95, 1–24.

Cookson, G., Pishue, B., 2017. *Inrix Global Traffic Scorecard*. INRIX Research.

Dantas, G., Siciliano, B., Freitas, L., Guedes de Seixas, E., da Silva, C.M., Arbilla, G., 2019. Why did ozone levels remain high in Rio de Janeiro during the Brazilian truck driver strike? *Atmospheric Pollut. Res.* 10 <https://doi.org/10.1016/j.apr.2019.09.010>, 2018–2029.

Deeter, M.N., Martínez-Alonso, S., Edwards, D.P., Emmons, L.K., Gille, J.C., Worden, H. M., Sweeney, C., Pittman, J.V., Daube, B.C., Wofsy, S.C., 2014. The MOPITT Version 6 product: algorithm enhancements and validation. *Atmospheric Meas. Tech.* 7, 3623–3632. <https://doi.org/10.5194/amt-7-3623-2014>.

ESA, 2020a. [https://www.esa.int/Applications/Observing\\_the\\_Earth/Copernicus/Sentinel-5P/COVID-19\\_nitrogen\\_dioxide\\_over\\_China](https://www.esa.int/Applications/Observing_the_Earth/Copernicus/Sentinel-5P/COVID-19_nitrogen_dioxide_over_China) accessed on 18 June 2020.

ESA, 2020b. [https://www.esa.int/Applications/Observing\\_the\\_Earth/Copernicus/Sentinel-5P/Coronavirus\\_lockdown\\_leading\\_to\\_drop\\_in\\_pollution\\_across\\_Europe](https://www.esa.int/Applications/Observing_the_Earth/Copernicus/Sentinel-5P/Coronavirus_lockdown_leading_to_drop_in_pollution_across_Europe) accessed on 18 June 2020.

Edwards, D.P., Halvorson, C.M., Gille, J.C., 1999. Radiative transfer modeling for the EOS terra satellite measurement of pollution in the troposphere (MOPITT) instrument. *J. Geophys. Res. Atmospheres* 104, 16755–16775. <https://doi.org/10.1029/1999JD900167>.

Freitas, E.D., Rozoff, C.M., Cotton, W.R., Dias, P.L.S., 2007. Interactions of an urban heat island and sea-breeze circulations during winter over the metropolitan area of São Paulo, Brazil. *Bound. -Layer Meteorol.* 122, 43–65. <https://doi.org/10.1007/s10546-006-9091-3>.

Global Energy Review, 2020. *The Impacts of the Covid-19 Crisis on Global Energy Demand and CO2 Emissions*. IEA, 2020.

Kalpasanov, Y., Kurchatova, G., 1976. A study of the statistical distribution of chemical pollutants in air. *J. Air Pollut. Contr. Assoc.* 26, 981–985. <https://doi.org/10.1080/00022470.1976.10470349>.

Kanniah, K.D., Kamarul Zaman, N.A.F., Kaskaoutis, D.G., Latif, M.T., 2020. COVID-19's impact on the atmospheric environment in the Southeast Asia region. *Sci. Total Environ.* 736, 139658. <https://doi.org/10.1016/j.scitotenv.2020.139658>.

Kawashima, A.B., Martins, L.D., Rafee, S.A.A., Rudke, A.P., de Moraes, M.V., Martins, J. A., 2020. Development of a spatialized atmospheric emission inventory for the main industrial sources in Brazil. *Environ. Sci. Pollut. Res.* (27), 35941–35951. <https://doi.org/10.1007/s11356-020-08281-7>.

Kristiansen, N.J., Stohl, A., Olivie, D.J.L., Croft, B., Søvde, O.A., Klein, H., Christoudias, T., Kunkel, D., Leadbetter, S.J., Lee, Y.H., Zhang, K., Tsigaridis, K., Bergman, T., Evangelisti, N., Wang, H., Ma, P.-L., Easter, R.C., Rasch, P.J., Liu, X., Pitari, G., Di Genova, G., Zhao, S.Y., Balkanski, Y., Bauer, S.E., Faluvegi, G.S., Kokkola, H., Martin, R.V., Pierce, J.R., Schulz, M., Shindell, D., Tost, H., Zhang, H., 2016. Evaluation of observed and modelled aerosol lifetimes using radioactive tracers of opportunity and an ensemble of 19 global models. *Atmos. Chem. Phys.* 16, 3525–3561. <https://doi.org/10.5194/acp-16-3525-2016>.

Le Quéré, C., Jackson, R.B., Jones, M.W., Smith, A.J.P., Abernethy, S., Andrew, R.M., DeGol, A.J., Willis, D.R., Shan, Y., Canadell, J.G., Friedlingstein, P., Creutzig, F., Peters, G.P., 2020. Temporary reduction in daily global CO<sub>2</sub> emissions during the COVID-19 forced confinement. *Nat. Clim. Change* 10, 647–653. <https://doi.org/10.1038/s41558-020-0797-x>.

Leirião, L.F.L., Miraglia, S.G.E.K., 2019. Environmental and health impacts due to the violation of Brazilian emissions control program standards in São Paulo Metropolitan Area. *Transp. Res. Part Transp. Environ.* 70, 70–76. <https://doi.org/10.1016/j.trd.2019.03.006>.

Leirião, L.F.L., Debone, D., Pauliquevis, T., Rosário, N.M.É. do, Miraglia, S.G.E.K., 2020. Environmental and public health effects of vehicle emissions in a large metropolis: case study of a truck driver strike in São Paulo, Brazil. *Atmospheric Pollut. Res.* 11, 24–31. <https://doi.org/10.1016/j.apr.2020.02.020>.

Levett, P.F., van den Oord, G.H.J., Dobber, M.R., Malkki, A., Visser, Huib, Johan de Vries, Stammes, P., Lundell, J.O.V., Saari, H., 2006. The ozone monitoring instrument. *IEEE Trans. Geosci. Rem. Sens.* 44, 1093–1101. <https://doi.org/10.1109/TGRS.2006.872333>.

Levy, I., 2013. A national day with near zero emissions and its effect on primary and secondary pollutants. *Atmos. Environ.* 77, 202–212. <https://doi.org/10.1016/j.atmosenv.2013.05.005>.

Levy, I., Mihele, C., Lu, G., Narayan, J., Hilker, N., Brook, J.R., 2014. Elucidating multipollutant exposure across a complex metropolitan area by systematic deployment of a mobile laboratory. *Atmos. Chem. Phys.* 14, 7173–7193. <https://doi.org/10.5194/acp-14-7173-2014>.

Li, J., Carlson, B.E., Lacis, A.A., 2015. How well do satellite AOD observations represent the spatial and temporal variability of PM 2.5 concentration for the United States? *Atmos. Environ. Times* 102, 260–273. <https://doi.org/10.1016/j.atmosenv.2014.12.010>.

Lima, F.D.M., Pérez-Martínez, P.J., de Fatima Andrade, M., Kumar, P., de Miranda, R.M., 2020. Characterization of particles emitted by pizzerias burning wood and briquettes: a case study at São Paulo, Brazil. *Environ. Sci. Pollut. Control Ser.* 1–14. <https://doi.org/10.1007/s11356-019-07508-6>.

Liu, Y., Zhao, N., Vanos, J.K., Cao, G., 2017. Effects of synoptic weather on ground-level PM 2.5 concentrations in the United States. *Atmos. Environ.* 148, 297–305. <https://doi.org/10.1016/j.atmosenv.2016.10.052>.

Mahalakshmi, D.V., Sujatha, P., Naidu, C.V., Chowdary, V.M., 2014. Contribution of vehicular emission on urban air quality: results from public strike in Hyderabad. *Indian J. Radio Space Phys.* 43, 340–348.

Mahato, S., Pal, S., Ghosh, K.G., 2020. Effect of lockdown amid COVID-19 pandemic on air quality of the megacity Delhi, India. *Sci. Total Environ.* 730, 139086. <https://doi.org/10.1016/j.scitotenv.2020.139086>.

Malik, L., Tiwari, G., Thakur, S., Kumar, A., 2019. Assessment of freight vehicles characteristics and impact of future policy interventions in Delhi. *Transp. Res. Part Transp. Environ.* 67, 610–627. <https://doi.org/10.1016/j.trd.2019.01.007>.

Mayer, H., 1999. Air pollution in cities. *Atmos. Environ.* 33, 4029–4037. [https://doi.org/10.1016/S1352-2310\(99\)00144-2](https://doi.org/10.1016/S1352-2310(99)00144-2).

Meinardi, S., Nissensohn, P., Barletta, B., Dabdub, D., Sherwood Rowland, F., Blake, D.R., 2008. Influence of the public transportation system on the air quality of a major urban center. A case study: milan, Italy. *Atmos. Environ.* 42, 7915–7923. <https://doi.org/10.1016/j.atmosenv.2008.07.046>.

Muhammad, S., Long, X., Salman, M., 2020. COVID-19 pandemic and environmental pollution: a blessing in disguise? *Sci. Total Environ.* 728, 138820. <https://doi.org/10.1016/j.scitotenv.2020.138820>.

Nakada, L.Y.K., Urban, R.C., 2020. COVID-19 pandemic: impacts on the air quality during the partial lockdown in São Paulo state. *Brazil. Sci. Total Environ.* 730, 139087. <https://doi.org/10.1016/j.scitotenv.2020.139087>.

NASA, 2020. <https://earthobservatory.nasa.gov/images> .(accessed on 18 june 2020).

Online pollutant database of the environmental agency of the state of São Paulo: <http://qualar.cetesb.sp.gov.br/qualar/home.do> (accessed on September 11, 2019).

Orlando, J.P., Alvim, D.S., Yamazaki, A., Corrêa, S.M., Gatti, L.V., 2010. Ozone precursors for the São Paulo metropolitan area. *Sci. Total Environ.* 408, 1612–1620. <https://doi.org/10.1016/j.scitotenv.2009.11.060>.

Paraiso, M.L. de S., Gouveia, N., 2015. Health risks due to pre-harvesting sugarcane burning in São Paulo State, Brazil. *Rev. Bras. Epidemiol.* 18, 691–701. <https://doi.org/10.1590/1980-5497201500030014>.

Pereira, G., Shimabukuro, Y.E., Moraes, E.C., Freitas, S.R., Cardozo, F.S., Longo, K.M., 2011. Monitoring the transport of biomass burning emission in South America. *Atmospheric Pollut. Res.* 2, 247–254. <https://doi.org/10.5094/APR.2011.031>.

Pereira, G.M., Teinilä, K., Custódio, D., Gomes Santos, A., Xian, H., Hillamo, R., Alves, C. A., Bittencourt de Andrade, J., Olímpio da Rocha, G., Kumar, P., Balasubramanian, R., Andrade, M. de F., de Castro Vasconcellos, P., 2017. Particulate pollutants in the Brazilian city of São Paulo: 1-year investigation for the chemical composition and source apportionment. *Atmos. Chem. Phys.* 17, 11943–11969. <https://doi.org/10.5194/acp-17-11943-2017>.

Platnick, S., King, M.D., Ackerman, S.A., Menzel, W.P., Baum, B.A., Riedi, J.C., Frey, R. A., 2003. The MODIS cloud products: algorithms and examples from terra. *IEEE Trans. Geosci. Rem. Sens.* 41, 459–473. <https://doi.org/10.1109/TGRS.2002.808301>.

Sánchez-Cocillo, O.R., de Fátima Andrade, M., 2002a. The influence of meteorological conditions on the behavior of pollutants concentrations in São Paulo, Brazil. *Environ. Pollut.* 116, 257–263. [https://doi.org/10.1016/S0269-7491\(01\)00129-4](https://doi.org/10.1016/S0269-7491(01)00129-4).

Sharma, A.R., Kharol, S.K., Badarinath, K.V.S., 2010. Influence of vehicular traffic on urban air quality – a case study of Hyderabad, India. *Transp. Res. Part Transp. Environ.* 15, 154–159. <https://doi.org/10.1016/j.trd.2009.11.001>.

Sharma, S., Zhang, M., Anshika, Gao, J., Zhang, H., Kota, S.H., 2020. Effect of restricted emissions during COVID-19 on air quality in India. *Sci. Total Environ.* 728, 138878. <https://doi.org/10.1016/j.scitotenv.2020.138878>.

Siciliano, B., Dantas, G., da Silva, C.M., Arbillia, G., 2020. Increased ozone levels during the COVID-19 lockdown: analysis for the city of Rio de Janeiro, Brazil. *Sci. Total Environ.* 737, 139765. <https://doi.org/10.1016/j.scitotenv.2020.139765>.

Sider, T., Hatzopoulou, M., Eluru, N., Goulet-Langlois, G., Manaugh, K., 2015. Smog and socioeconomics: an evaluation of equity in traffic-related air pollution generation and exposure. *Environ. Plann. Plann. Des.* 42, 870–887. <https://doi.org/10.1068/b130140p>.

Silva, C.B.P. da, Saldiva, P.H.N., Amato-Lourenço, L.F., Rodrigues-Silva, F., Miraglia, S.G. E.K., 2012. Evaluation of the air quality benefits of the subway system in São Paulo, Brazil. *J. Environ. Manag.* 101, 191–196. <https://doi.org/10.1016/j.jenvman.2012.02.009>.

Tobías, A., Carnerero, C., Reche, C., Massagué, J., Via, M., Minguillón, M.C., Alastuey, A., Querol, X., 2020. Changes in air quality during the lockdown in Barcelona (Spain) one month into the SARS-CoV-2 epidemic. *Sci. Total Environ.* 726, 138540. <https://doi.org/10.1016/j.scitotenv.2020.138540>.

Vieira-Filho, M.S., Lehmann, C., Fornaro, A., 2015. Influence of local sources and topography on air quality and rainwater composition in Cubatão and São Paulo, Brazil. *Atmos. Environ.* 101, 200–208. <https://doi.org/10.1016/j.atmosev.2014.11.025>.

WHO (Ed.), 2000. Air Quality Guidelines for Europe, 2. Ed. Ed, WHO Regional Publications European Series. World Health Organization, Regional Office for Europe, Copenhagen.

Wu, X., Nethery, R.C., Sabath, B.M., Braun, D., Dominici, F., 2020. Air pollution and COVID-19 mortality in the United States: Strengths and limitations of an ecological regression analysis. *Science Advances* 6 (45), 1–7. <https://doi.org/10.1126/sciadv.abd4049>. In this issue.

Zambrano-Monserrate, M.A., Ruano, M.A., Sanchez-Alcalde, L., 2020. Indirect effects of COVID-19 on the environment. *Sci. Total Environ.* 728, 138813. <https://doi.org/10.1016/j.scitotenv.2020.138813>.